

JLab Measurement of the ^4He Charge Form Factor at Large Momentum Transfers

A. Camsonne²², A.T. Katramatou¹¹, M. Olson²⁰, N. Sparveris^{11,21}, A. Acha⁴, K. Allada¹², B.D. Anderson¹¹, J. Arrington¹, A. Baldwin¹¹, J.-P. Chen²², S. Choi¹⁸, E. Chudakov²², E. Cisbani^{8,10}, B. Craver²³, P. Decowski¹⁹, C. Dutta¹², E. Folts²², S. Frullani^{8,10}, F. Garibaldi^{8,10}, R. Gilman^{16,22}, J. Gomez²², B. Hahn²⁴, J.-O. Hansen²², D. Higinbotham²², T. Holmstrom¹³, J. Huang¹⁴, M. Iodice⁹, X. Jiang¹⁶, A. Kelleher²⁴, E. Khrosinkova¹¹, A. Kievsky⁷, E. Kuchina¹⁶, G. Kumbartzki¹⁶, B. Lee¹⁸, J.J. LeRose²², R.A. Lindgren²³, G. Lott²², H. Lu¹⁷, L.E. Marcucci^{7,15}, D.J. Margaziotis², P. Markowitz⁴, S. Marrone⁶, D. Meekins²², Z.-E. Meziani²¹, R. Michaels²², B. Moffit¹⁴, B. Norum²³, G.G. Petratos¹¹, A. Puckett¹⁴, X. Qian³, O. Rondon²³, A. Saha²², B. Sawatzky²¹, J. Segal²², M. Shabestari²³, A. Shahinyan²⁵, P. Solvignon¹, R.R. Subedi²³, R. Suleiman²², V. Sulkosky²², G.M. Urciuoli⁸, M. Viviani⁷, Y. Wang⁵, B.B. Wojtsekhowski²², X. Yan¹⁸, H. Yao²¹, W.-M. Zhang¹¹, X. Zheng²³, L. Zhu⁵

¹Argonne National Laboratory, Argonne, IL 60439, USA

²California State University, Los Angeles, CA 90032, USA

³Duke University (TUNL), Durham, NC 27708, USA

⁴Florida International University, Miami, FL 33199, USA

⁵University of Illinois at Urbana Champagne, Urbana, IL 61801, USA

⁶Istituto Nazionale di Fisica Nucleare, Sezione di Bari and University of Bari, 70126 Bari, Italy

⁷Istituto Nazionale di Fisica Nucleare, Sezione di Pisa, 56127 Pisa, Italy

⁸Istituto Nazionale di Fisica Nucleare, Sezione di Roma, 00185 Rome, Italy

⁹Istituto Nazionale di Fisica Nucleare, Sezione di Roma Tre, 00146 Rome, Italy

¹⁰Istituto Superiore di Sanità, 00161 Rome, Italy

¹¹Kent State University, Kent OH 44242, USA

¹²University of Kentucky, Lexington, KY 40506, USA

¹³Longwood University, Farmville, VA 23909, USA

¹⁴Massachusetts Institute of Technology, Cambridge, MA 02139, USA

¹⁵University of Pisa, 56127 Pisa, Italy

¹⁶Rutgers, The State University of New Jersey, Piscataway, NJ 08855, USA

¹⁷University of Science and Technology of China, Hefei, Anhui, 230026 P.R. China

¹⁸Seoul National University, Seoul 151-747, Korea

¹⁹Smith College, Northampton, MA 01063, USA

²⁰St. Norbert College, De Pere WI 54115, USA

²¹Temple University, Philadelphia, PA 19122, USA

²²Thomas Jefferson National Accelerator Facility, Newport News, VA 23606, USA

²³University of Virginia, Charlottesville, VA 22901, USA

²⁴College of William and Mary, Williamsburg, VA 23185, USA and

²⁵Yerevan Physics Institute, Yerevan 375036, Armenia

(Dated: September 10, 2013; The Jefferson Lab Hall A Collaboration)

The charge form factor of ^4He has been extracted in the range $29 \text{ fm}^{-2} \leq Q^2 \leq 77 \text{ fm}^{-2}$ from elastic electron scattering, detecting ^4He nuclei and electrons in coincidence with the High Resolution Spectrometers of the Hall A Facility of Jefferson Lab. The results are in qualitative agreement with realistic meson-nucleon theoretical calculations. The data have uncovered a second diffraction minimum, which was predicted in the Q^2 range of this experiment, and rule out conclusively long-standing predictions of dimensional scaling of high-energy amplitudes using quark counting.

PACS numbers: 25.30.Bf, 13.40.Gp, 27.10.+h, 24.85.+p

The electromagnetic (EM) form factors of the helium isotopes are, along with the deuteron and tritium form factors, the “observables of choice” [1] for testing the nucleon-meson standard model of the nuclear interaction and the associated EM current operator [2]. They provide fundamental information on the internal structure and dynamics of the light nuclei as they are, in a simple picture, convolutions of the ground state wave function with the EM form factors of the constituent nucleons. The theoretical calculations for these few-body observables are very sensitive to the model used for the nuclear EM current operator, especially its meson-

exchange-current (MEC) contributions. Relativistic corrections and possible admixtures of multi-quark states in the nuclear wave function might also be relevant [2]. Additionally, at large momentum transfers, these EM form factors may offer a unique opportunity to uncover a possible transition in the description of elastic electron scattering on few-body nuclear systems, from meson-nucleon to quark-gluon degrees of freedom, as predicted by quark-dimensional scaling [3, 4].

Experimentally, the few-body form factors are determined from elastic electron-nucleus scattering studies using high intensity beams, high density targets and large

solid angle magnetic spectrometers. There have been extensive experimental investigations of the few-body form factors over the past 50 years at almost every electron accelerator laboratory [5, 6], complemented by equally extensive theoretical calculations and predictions [2, 6].

This work focuses on a measurement of the ^4He charge form factor, F_c , at large momentum transfers, at Jefferson Lab (JLab). The cross section for elastic scattering of a relativistic electron from the spin zero ^4He nucleus is given, in the one-photon (between electron and nucleus) exchange approximation, by the formula [7]:

$$\frac{d\sigma}{d\Omega}(E, \theta) = \frac{(Z\alpha)^2 E' \cos^2(\frac{\theta}{2})}{4E^3 \sin^4(\frac{\theta}{2})} F_c^2(Q^2), \quad (1)$$

where α is the fine-structure constant, Z is the nuclear charge, E and E' are the incident and scattered electron energies, θ is the electron scattering angle, and $Q^2 = 4EE' \sin^2(\theta/2)$ is the four-momentum transfer squared.

The few-body EM form factors have been theoretically investigated by several groups, using different techniques to solve for the nuclear ground states, and a variety of models for the nuclear EM current. The most recent calculation of ^3H and ^3He EM form factors is that of Refs. [1, 8]. It uses the pair-correlated hyperspherical harmonics (HH) method [9] to obtain the few-body nuclear wave functions and goes beyond the impulse approximation (IA), where the electron interacts with one of the nucleon constituents, by including MEC, whose main contributions are constructed to satisfy the current conservation relation with the given Hamiltonian [8]. Part of the present work is the extension of the above method to the ^4He charge form factor (see Figs. 1 and 2) by using the (uncorrelated) HH expansion to solve for the ^4He wave function from the Argonne AV18 [10] nucleon-nucleon (NN) and Urbana IX [11] three-nucleon ($3N$) interactions, and including MEC contributions arising from π -, ρ - and ω -meson exchanges, as well as the $\rho\pi\gamma$ and $\omega\pi\gamma$ charge transition couplings. For more details, the reader is referred to Ref. [9] for the HH method, and Refs. [1, 8] for the nuclear EM current model. The present experimental and theoretical results are compared to (see below) (i) the Monte Carlo calculations of Refs. [12, 13], where the variational Monte Carlo (VMC) and the Green's function Monte Carlo (GFMC) methods were used to solve for the ^4He wave function, and (ii) the long-standing prediction of the dimensional-scaling quark model (DSQM) approach of Ref. [3].

In fact, at large momentum transfers, elastic scattering from few-body nuclear systems like ^4He may be partly due to, or even dominated by, contributions from electron interaction with the nucleons' constituent quarks. Several groups have developed purely phenomenological "hybrid quark-hadron" models that include multi-quark states for overlapping nucleons in the nuclear wave function, which augment the IA calculated form factors [14]. On the other hand, the DSQM approach incorporates the nucleon's quark-gluon substructure in elastic electron scattering from few-body systems by applying di-

mensional scaling of high energy amplitudes using quark counting. This leads to the prediction for the ^4He case that $\sqrt{F_c(Q^2)} \sim (Q^2)^{1-3A}$, where $A = 4$, and to the dominance of the constituent-interchange force between quarks of different nucleons to share Q/A (see Ref. [3]).

The experiment (E04-018) used the Continuous Electron Beam (100% duty factor) Accelerator and Hall A Facilities of JLab. Electrons scattered from a high density cryogenic ^4He target were detected in the Left High Resolution Spectrometer (e-HRS). To suppress backgrounds and unambiguously separate elastic from inelastic processes, recoil helium nuclei were detected in the Right HRS (h-HRS) in coincidence with the scattered electrons.

The energy of the incident beam ranged between 2.09 and 4.13 GeV. The beam current was measured using two resonant cavity current monitors upstream of the target. It ranged, on average for different kinematical settings, between 38 and 82 μA . The two cavities were calibrated against a parametric current transformer monitor (Unser monitor). To reduce beam-induced target density changes and to avoid possible destruction of the target cell, the beam was rastered on the target in both horizontal and vertical directions at high frequency, resulting in an effective beam spot size of $2 \times 2 \text{ mm}^2$.

The target system contained gaseous ^4He and liquid hydrogen cells of length $T=20 \text{ cm}$. The ^4He gas was pressurized to 13.7-14.2 atm at a temperature of 7.14-8.68 K, resulting in a density of 0.102-0.127 g/cm^3 . Two Al foils separated by 20 cm were used to measure any possible contribution to the cross section from the Al end-caps of the target cells. This system provided, at the maximum beam current of 110 μA , a record high luminosity of $2.7 \times 10^{38} \text{ cm}^{-2}\text{s}^{-1}$, for the ^4He target.

Scattered electrons were detected in the e-HRS using two planes of scintillators to form an "electron" trigger, a pair of drift chambers for electron track reconstruction, and a gas threshold Čerenkov counter and a lead-glass calorimeter for electron identification. Recoil nuclei were detected in the h-HRS using two planes of scintillators to form a "recoil" trigger and a pair of drift chambers for recoil track reconstruction. The event trigger consisted of a coincidence between the two HRS triggers. Details on the Hall A Facility and all associated beam, target and spectrometer apparatuses used are given in Ref. [15].

Particles in the e-HRS were identified as electrons on the basis of a minimal pulse height in the Čerenkov counter ("Čerenkov cut") and the energy deposited in the calorimeter, consistent with the momentum as determined from the drift chamber track using the spectrometer's optical properties ("calorimeter cut"). Particles in the h-HRS were identified as ^4He on the basis of their energy deposition (pulse height) in the first scintillator hodoscope ("helium cut"). Electron- ^4He (e - ^4He) coincidence events were identified using the relative time-of-flight (TOF) between the electron and recoil triggers after imposing the above three cuts. To check the overall normalization, elastic electron-proton (e - p) scattering was measured at several kinematics with solid angle Ja-

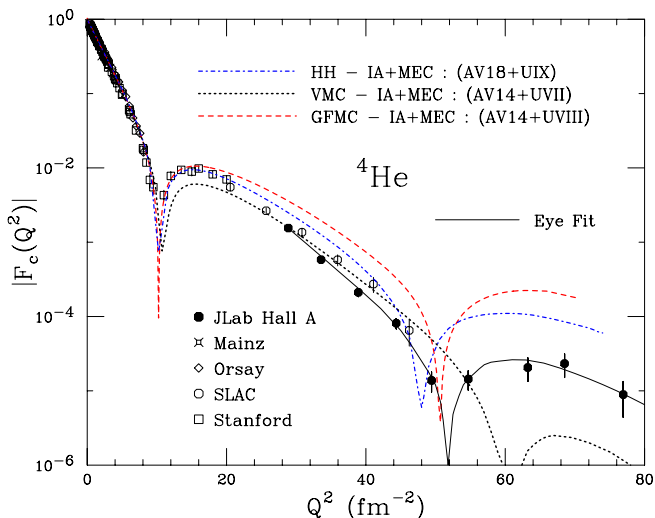


FIG. 1. ${}^4\text{He}$ charge form factor data from this experiment are compared with the present HH theoretical IA+MEC calculation using the AV18+Urbana IX Hamiltonian model. Also shown are previous Stanford, Orsay, Mainz and SLAC data, and older VMC and GFMC theoretical calculations (see text). The solid line has been drawn to just guide the eye.

cobians similar to those for $e^{-4}\text{He}$ elastic scattering. The e - p measured cross section values were found to be in excellent agreement (to within $\pm 2.0\%$) with values calculated using a proton form factor fit [16] based on all existing e - p elastic cross section measurements.

The elastic $e^{-4}\text{He}$ cross section values were calculated using the formula:

$$\frac{d\sigma}{d\Omega}(E, \theta) = \frac{N_{er} C_{cor}}{N_b N_t (\Delta\Omega)_{MC} F(Q^2, T)}, \quad (2)$$

where N_{er} is the number of electron-recoil ${}^4\text{He}$ elastic events, N_b is the number of incident beam electrons, N_t is the number of target nuclei/cm 2 , $(\Delta\Omega)_{MC}$ is the effective coincidence solid angle (which includes most radiative effects) from a Monte Carlo simulation, F is the portion of the radiative corrections that depends only on Q^2 and T (1.10 on average) [17], and $C_{cor} = C_{det} C_{cdt} C_{rni} C_{den}$. Here, C_{det} is the correction for the inefficiency of the Čerenkov counter and the calorimeter (1.01%) (the scintillator counter hodoscopes and the drift chamber sets were found to be essentially 100% efficient), C_{cdt} is the computer dead-time correction (between 1.05 and 1.17), C_{rni} is a correction for losses of recoil nuclei due to nuclear interactions in the target cell and vacuum windows [1.10(1.03) at the lowest(highest) Q^2], and C_{den} is a correction to the target density due to beam heating effects (ranging between 1.03 at 38 μA and 1.06 at 82 μA). There were no contributions to the elastic $e^{-4}\text{He}$ cross section from events originating in the target cell end-caps, as determined from runs with the empty replica target. The e - p elastic cross section values were determined similarly.

The effective coincidence solid angle was evaluated with a Monte Carlo computer code that simulated elastic electron-nucleus scattering under identical conditions

Q^2 fm $^{-2}$	E GeV	θ deg.	$d\sigma/d\Omega$ cm 2 /sr	$ F_c $
28.87	2.091	30.52	$(2.04 \pm 0.18) \times 10^{-36}$	$(1.55 \pm 0.07) \times 10^{-3}$
33.56	2.091	33.20	$(1.99 \pm 0.22) \times 10^{-37}$	$(5.77 \pm 0.32) \times 10^{-4}$
38.92	2.091	36.11	$(1.69 \pm 0.42) \times 10^{-39}$	$(2.01 \pm 0.23) \times 10^{-4}$
44.36	4.048	19.25	$(9.51 \pm 2.76) \times 10^{-39}$	$(8.01 \pm 0.12) \times 10^{-5}$
49.43	4.048	20.40	$(2.14 \pm 1.01) \times 10^{-40}$	$(1.36 \pm 0.32) \times 10^{-5}$
54.71	4.048	21.56	$(1.87 \pm 0.88) \times 10^{-40}$	$(1.42 \pm 0.33) \times 10^{-5}$
63.23	4.127	22.86	$(2.84 \pm 1.91) \times 10^{-40}$	$(2.02 \pm 0.68) \times 10^{-5}$
68.51	4.127	23.90	$(2.97 \pm 1.99) \times 10^{-40}$	$(2.26 \pm 0.76) \times 10^{-5}$
76.95	4.127	25.50	$(3.31 \pm 3.38) \times 10^{-41}$	$(8.67 \pm 4.43) \times 10^{-6}$

TABLE I. Kinematics, elastic $e^{-4}\text{He}$ cross section and ${}^4\text{He}$ charge form factor results from this experiment, and total errors (statistical and systematic added in quadrature).

as our measurements. The code tracked scattered electrons and recoil nuclei from the target to the detectors through the two HRS systems using optical models based on magnetic field measurements and precision position surveys of their elements. The effects from ionization energy losses and multiple scattering in the target and vacuum windows were taken into account for both electrons and recoil nuclei. Bremsstrahlung radiation losses for both incident and scattered electrons in the target and vacuum windows, as well as internal radiative effects, were also taken into account. Details on this simulation method can be found in Ref. [17]. Monte Carlo simulated spectra of scattered electrons and recoil nuclei were found to be in very good agreement with experimentally measured spectra.

The extracted ${}^4\text{He}$ charge form factor (absolute) values are listed in Table I, and shown in Fig. 1 along with previous Stanford [18], Orsay [19], SLAC [20] and Mainz [21] data. The error bars in Fig. 1 represent statistical and systematic uncertainties added in quadrature. The solid

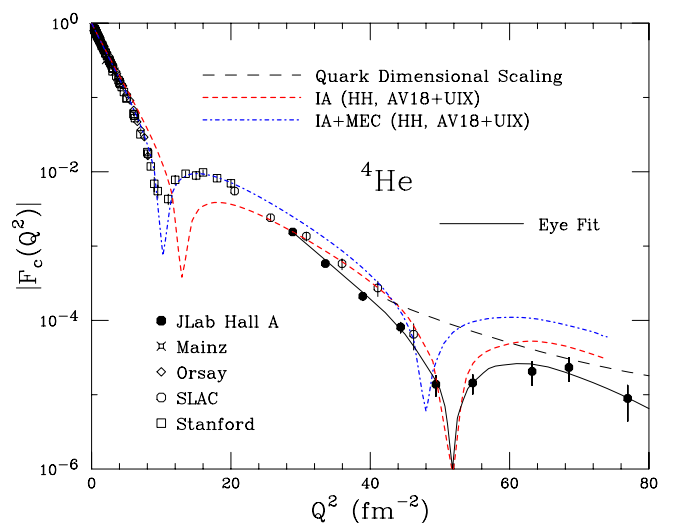


FIG. 2. ${}^4\text{He}$ charge form factor data from this experiment are compared to both IA and IA+MEC HH present calculations, which use the AV18+Urbana IX Hamiltonian model, and to the DSQM prediction (see text). Also shown are the previous Stanford, Orsay, Mainz and SLAC data.

curve in Fig. 1 labeled as “eye fit” is a line drawn just to guide the eye. The new data in the figure suggest the existence of a second diffraction minimum for the ${}^4\text{He}$ form factor at $Q^2 = (51.7 \pm 0.2) \text{ fm}^{-2}$. The existence of the minimum is confirmed by the momentum distribution of the observed $e^{-4}\text{He}$ elastic events for the two Q^2 points about the minimum, 50 and 55 fm^{-2} : for the former (latter) point, the distribution is indicative of a fast falling (rising) form factor with Q^2 . It is also evident from Fig. 1 that the new JLab data are in significant disagreement with the existing SLAC data.

The data in Fig. 1 are compared to the HH variational calculation performed using the AV18 NN and Urbana IX $3N$ interactions. Also shown are the VMC results of Ref. [12], obtained with the older Argonne AV14 NN and Urbana VII $3N$ interaction, and the GFMC results of Ref. [13], obtained with the AV14 and Urbana VIII $3N$ force model. It can be seen that all three calculations, which include MEC contributions, are in qualitative agreement with the new JLab data and do predict, though at different locations, a second diffraction minimum for $Q^2 > 40 \text{ fm}^{-2}$. The present HH calculation for the ${}^4\text{He}$ F_c is in a qualitatively better agreement with the data when compared with the older Monte Carlo studies of Refs. [12, 13]. To better investigate this aspect, we show in Fig. 2 the experimental data along with the HH results, with and without (IA only) inclusion of MEC. Of note is that the lower Q^2 data are in good agreement with the calculation that includes MEC, while the higher Q^2 data are in better agreement with the IA only calculation. This observation may be indicative of a possible diminishing role of MEC with increasing Q^2 required to bring the theory into better agreement with the data. The inadequacy of the above theoretical approach to de-

scribe well the entire Q^2 range of the ${}^4\text{He}$ F_c may also indicate the need for a truly covariant relativistic framework, which has been successful in describing all deuteron form factor data [6]. In fact, we would like to remark that the second diffraction minimum is in a range of Q^2 where the applicability of the standard non-relativistic nuclear physics approach presented here may be questionable.

Also shown in Fig. 2 is the asymptotic prediction of the dimensional-scaling quark model by Brodsky and Chertok [3], arbitrarily normalized at $Q^2 = 40 \text{ fm}^{-2}$. It is evident that the data rule out conclusively the applicability of the long-standing quark dimensional scaling prediction for elastic electron- ${}^4\text{He}$ scattering, at least in the Q^2 range accessible by the JLab accelerator.

In summary, we have measured the ${}^4\text{He}$ charge form factor in the range $29 \text{ fm}^{-2} \leq Q^2 \leq 77 \text{ fm}^{-2}$. The new data have uncovered a second diffraction minimum for this form factor. They constrain inherent uncertainties of the theoretical calculations and lead, together with previous large Q^2 data on the deuteron, ${}^3\text{He}$ and tritium elastic form factors [20, 22, 23], to the development of a consistent hadronic model describing the internal EM structure and dynamics of few-body nuclear systems.

We acknowledge the outstanding support of the staff of the Accelerator and Physics Divisions of JLab that made this experiment possible. We are grateful to Drs. D. Riska, R. Schiavilla and R. Wiringa for kindly providing their theoretical calculations, and to Drs. F. Gross and R. Schiavilla for valuable discussions and support. This work was supported in part by the U.S. Department of Energy and National Science Foundation, including grants DE-AC05-06OR23177, DE-AC02-06CH11357, DE-FG02-96ER40950, NSF-PHY-0701679 and NSF-PHY-0652713, the Kent State University Research Council and the Italian Institute for Nuclear Research.

-
- [1] L. E. Marcucci, D. O. Riska, and R. Schiavilla, *Phys. Rev.* **C58**, 3069 (1998).
 - [2] J. Carlson and R. Schiavilla, *Rev. Mod. Phys.* **70**, 743 (1998); and references therein.
 - [3] S. J. Brodsky and B. T. Chertok, *Phys. Rev.* **D14**, 3003 (1976); B. T. Chertok, *Phys. Rev. Lett.* **41**, 1155 (1978).
 - [4] C. E. Carlson, J. R. Hiller, and R. J. Holt, *Annu. Rev. Nucl. Part. Sci.* **47**, 395 (1997); R. J. Holt and R. Gilman, *Rept. Prog. Phys.* **75**, 086301 (2012).
 - [5] I. Sick, *Prog. Part. Nucl. Phys.* **47**, 245 (2001).
 - [6] R. Gilman and F. Gross, *J. Phys.* **G28**, R37 (2002).
 - [7] S. D. Drell and J. D. Walecka, *Ann. Phys. (N.Y.)* **28**, 18 (1964).
 - [8] L. E. Marcucci *et al.*, *Phys. Rev.* **C72**, 014001 (2005).
 - [9] A. Kievsky *et al.*, *J. Phys.* **G35**, 063101 (2008); and references therein.
 - [10] R. B. Wiringa, V. G. J. Stoks, and R. Schiavilla, *Phys. Rev.* **C51**, 38 (1995).
 - [11] B. S. Pudliner *et al.*, *Phys. Rev. Lett.* **74**, 4396 (1995).
 - [12] R. Schiavilla, V. R. Pandharipande, and D. O. Riska, *Phys. Rev.* **C41**, 309 (1990).
 - [13] R. B. Wiringa, *Phys. Rev.* **C43**, 1585 (1991).
 - [14] M. Namiki, K. Okano, and N. Oshimo, *Phys. Rev.* **C25**, 2157 (1982). V. V. Burov and V. K. Lukyanov, *Nucl. Phys.* **A463**, 263c (1987).
 - [15] J. Alcorn *et al.*, *Nucl. Instrum. Methods* **A522**, 294 (2004).
 - [16] J. Arrington, W. Melnitchouk, and J. A. Tjon, *Phys. Rev.* **C76**, 035205 (2007).
 - [17] A. T. Katramatou, Kent State University preprint KSU-CNR-14-11, December 2011.
 - [18] R. F. Frosch *et al.*, *Phys. Rev.* **160**, 874 (1967); J. S. McCarthy, I. Sick, and R. R. Whitney, *Phys. Rev.* **C15**, 1396 (1977).
 - [19] J. P. Repellin *et al.*, *Phys. Lett.* **B16**, 169 (1965).
 - [20] R. G. Arnold *et al.*, *Phys. Rev. Lett.* **40**, 1429 (1978).
 - [21] C. R. Ottermann *et al.*, *Nucl. Phys.* **A436**, 688 (1985).
 - [22] L. C. Alexa *et al.*, *Phys. Rev. Lett.* **82** 1374 (1999); P. E. Bosted *et al.*, *Phys. Rev.* **C42**, 38 (1990); D. Abbott *et al.*, *Phys. Rev. Lett.* **84**, 5053 (2000).
 - [23] A. Amroun *et al.*, *Nucl. Phys.* **A579**, 596 (1994); I. Nakagawa *et al.*, *Phys. Rev. Lett.* **86**, 5446 (2001).